



Optimized Schwarz Methods for curl-curl time-harmonic Maxwell's equations

Victorita Dolean, Martin J. Gander, Stéphane Lanteri, Jin-Fa Lee, Zhen Peng

► To cite this version:

Victorita Dolean, Martin J. Gander, Stéphane Lanteri, Jin-Fa Lee, Zhen Peng. Optimized Schwarz Methods for curl-curl time-harmonic Maxwell's equations. 2013. hal-00830282

HAL Id: hal-00830282

<https://hal.science/hal-00830282>

Preprint submitted on 4 Jun 2013

HAL is a multi-disciplinary open access archive for the deposit and dissemination of scientific research documents, whether they are published or not. The documents may come from teaching and research institutions in France or abroad, or from public or private research centers.

L'archive ouverte pluridisciplinaire **HAL**, est destinée au dépôt et à la diffusion de documents scientifiques de niveau recherche, publiés ou non, émanant des établissements d'enseignement et de recherche français ou étrangers, des laboratoires publics ou privés.

Optimized Schwarz Methods for curl-curl time-harmonic Maxwell's equations

Victorita Dolean^{1,2}, Martin J. Gander², Stéphane Lanteri³, Jin-Fa Lee⁴, and Zhen Peng⁴

1 Introduction

Like the Helmholtz equation, the high frequency time-harmonic Maxwell's equations are difficult to solve by classical iterative methods. Domain decomposition methods are currently most promising: following the first provably convergent method in [4], various optimized Schwarz methods were developed over the last decade [2, 3, 10, 11, 1, 6, 13, 14, 16, 8]. There are however two basic formulations for Maxwell's equation: the first order formulation, for which complete optimized results are known [6], and the second order, or curl-curl formulation, with partial optimization results [1, 13, 16]. We show in this paper that the convergence factors and the optimization process for the two formulations are the same. We then show by numerical experiments that the Fourier analysis predicts very well the behavior of the algorithms for a Yee scheme discretization, which corresponds to Nedelec edge elements on a tensor product mesh, in the curl-curl formulation. When using however mixed type Nedelec elements on an irregular tetrahedral mesh, numerical experiments indicate that transverse magnetic (TM) modes are less well resolved for high frequencies than transverse electric (TE) modes, and a heuristic can then be used to compensate for this in the optimization.

2 Optimized Schwarz algorithms

We consider the curl-curl problem in a bounded domain Ω , with boundary conditions on $\partial\Omega$ such that the problem is well posed [12]. A general Schwarz algorithm then solves for $n = 1, 2, \dots$ and the decomposition $\Omega = \Omega_1 \cup \Omega_2$ the subdomain problems

$$\begin{aligned} -\omega^2 \mathbf{E}^{1,n} + \nabla \times (\nabla \times \mathbf{E}^{1,n}) &= -i\omega \mathbf{Z} \mathbf{J} \quad \text{in } \Omega_1 \\ \mathcal{T}_{\mathbf{n}_1}(\mathbf{E}^{1,n}) &= \mathcal{T}_{\mathbf{n}_1}(\mathbf{E}^{2,n-1}) \quad \text{on } \partial\Omega_1 \cap \Omega_2, \\ -\omega^2 \mathbf{E}^{2,n} + \nabla \times (\nabla \times \mathbf{E}^{2,n}) &= -i\omega \mathbf{Z} \mathbf{J} \quad \text{in } \Omega_2 \\ \mathcal{T}_{\mathbf{n}_2}(\mathbf{E}^{2,n}) &= \mathcal{T}_{\mathbf{n}_2}(\mathbf{E}^{1,n-1}) \quad \text{on } \partial\Omega_2 \cap \Omega_1, \end{aligned} \tag{1}$$

University of Nice-Sophia Antipolis, France dolean@unice.fr · University of Geneva, Switzerland martin.gander@unige.ch · Inria Sophia Antipolis-Méditerranée, France Stephane.Lanteri@inria.fr · Ohio State University, ElectroScience Laboratory jinlee@esl.eng.ohio-state.edu; peng.98@osu.edu

where $\Gamma_{12} = \partial\Omega_1 \cap \Omega_2$, $\Gamma_{21} = \partial\Omega_2 \cap \Omega_1$, and $\mathcal{T}_{\mathbf{n}_j}$ are transmission conditions. The classical Schwarz method uses for example the impedance condition $\mathcal{T}_{\mathbf{n}}(\mathbf{E}) = (\nabla \times \mathbf{E} \times \mathbf{n}) \times \mathbf{n} + i\omega \mathbf{E} \times \mathbf{n}$, where \mathbf{n} denotes the unit outward normal.

The transmission conditions in [6] for the first order formulation, for which complete optimization results are available, can be written for the curl-curl formulation in the form

$$\mathcal{T}_{\mathbf{n}}^{DGG}(\mathbf{E}) = (I + \gamma_1(\mathcal{S}_{TM} + \mathcal{S}_{TE}))(\nabla \times \mathbf{E} \times \mathbf{n}) \times \mathbf{n} + i\omega(I - \gamma_1(\mathcal{S}_{TM} + \mathcal{S}_{TE}))(\mathbf{E} \times \mathbf{n}), \quad (2)$$

where $\mathcal{S}_{TM} = \nabla_{\tau} \nabla_{\tau} \cdot$, $\mathcal{S}_{TE} = \nabla_{\tau} \times \nabla_{\tau} \times$ and τ denotes the tangential direction. These transmission conditions are a particular case of the more general formulation

$$\begin{aligned} \mathcal{T}_{\mathbf{n}}^1(\mathbf{E}) = & (I + v_1(\delta_1 \mathcal{S}_{TM} + \delta_2 \mathcal{S}_{TE}))(\nabla \times \mathbf{E} \times \mathbf{n}) \times \mathbf{n} \\ & + i\omega(I - v_2(\delta_3 \mathcal{S}_{TM} + \delta_4 \mathcal{S}_{TE}))(\mathbf{E} \times \mathbf{n}), \end{aligned} \quad (3)$$

since by choosing $\delta_1 = \delta_2 = \delta_3 = \delta_4 = 1$, $v_1 = v_2 = \gamma_1$ in (3) we obtain (2).

Rawat and Lee proposed in [16] a transmission condition of the form

$$\begin{aligned} \mathcal{T}_{\mathbf{n}}^{RL}(\mathbf{E}) = & \mathbf{n} \times \nabla \times \mathbf{E} + \alpha \mathbf{n} \times (\mathbf{E} \times \mathbf{n}) + \beta \nabla_{\tau} \times \nabla_{\tau} \times (\mathbf{n} \times \mathbf{E} \times \mathbf{n}) + \gamma \nabla_{\tau} \nabla_{\tau} \cdot \mathbf{n} \times (\nabla \times \mathbf{E}) \\ = & (I + \gamma \mathcal{S}_{TM})(\mathbf{n} \times \nabla \times \mathbf{E}) + (\alpha + \beta \mathcal{S}_{TE})(\mathbf{n} \times (\mathbf{E} \times \mathbf{n})), \end{aligned} \quad (4)$$

and analyzed the performance for the case of plane waves traveling in the yz plane and with the interface in the xy plane. A different choice of transmission conditions was proposed in [13],

$$\begin{aligned} \mathcal{T}_{\mathbf{n}}^{TETM}(\mathbf{E}) = & (I - \gamma_2(\delta_1 \mathcal{S}_{TM} + \mathcal{S}_{TE}))(\mathbf{n} \times \nabla \times \mathbf{E}) \\ & + i\omega(-I + \gamma_2(\mathcal{S}_{TM} + \delta_4 \mathcal{S}_{TE}))(\mathbf{n} \times (\mathbf{E} \times \mathbf{n})). \end{aligned} \quad (5)$$

Both transmission conditions (4) and (5) are a particular case of the more general formulation

$$\begin{aligned} \mathcal{T}_{\mathbf{n}}^2(\mathbf{E}) = & (I + v_1(\delta_1 \mathcal{S}_{TM} + \delta_2 \mathcal{S}_{TE}))(\mathbf{n} \times \nabla \times \mathbf{E}) \\ & + i\omega(-I + v_2(\delta_3 \mathcal{S}_{TM} + \delta_4 \mathcal{S}_{TE}))(\mathbf{n} \times (\mathbf{E} \times \mathbf{n})), \end{aligned} \quad (6)$$

since by taking $\delta_1 = \delta_4 = 1$, $\delta_2 = \delta_3 = 0$, $v_1 = \gamma$, $v_2 = \beta$ in (6) we obtain (4), and choosing $\delta_2 = \delta_3 = 1$, $v_1 = -\gamma_2$, $v_2 = \gamma_2$ in (6) we obtain (5).

Thus, at first sight, it seems that there are two different classes of optimized algorithms, the ones with transmission conditions (3), and the ones with (6). One can show however that the optimized algorithm with the special form (2) of the transmission conditions (3) has identical convergence properties to the algorithm with transmission conditions (6) when taking $\delta_1 = \delta_2 = \delta_3 = \delta_4 = 1$, $v_1 = v_2 = -\gamma_1$ in (6), see [5]. In the following we will thus simply denote $\mathcal{T}_{\mathbf{n}}^2$ by $\mathcal{T}_{\mathbf{n}}$ and only study that case.

3 Convergence analysis using the TE-TM decomposition

We use Fourier analysis, and thus assume that the coefficients are constant, and the domain on which the original problem is posed is $\Omega = \mathbb{R}^3$, in which case we need the Silver-Müller radiation condition $\lim_{r \rightarrow \infty} r(\nabla \times E \times \mathbf{n} + i\omega \mathbf{E}) = 0$, where $r = |\mathbf{x}|$, $\mathbf{n} = \mathbf{x}/|\mathbf{x}|$, in order to obtain well-posed problems [12]. The two subdomains are now half spaces, $\Omega_1 = (0, \infty) \times \mathbb{R}^2$, $\Omega_2 = (-\infty, L) \times \mathbb{R}^2$, the interfaces are $\Gamma_{12} = \{L\} \times \mathbb{R}^2$ and $\Gamma_{21} = \{0\} \times \mathbb{R}^2$, and the overlap is $L \geq 0$. Let the Fourier transform in y and z directions be $\mathcal{F}\mathbf{E}(x, y, z) = \int_{\mathbb{R}^2} \mathbf{E}(x, y, z) e^{i(k_y y + k_z z)} dy dz$, where we denote by k_y and k_z the Fourier variables and $|\mathbf{k}|^2 = k_y^2 + k_z^2$. We first compute the local solutions of the homogeneous counterparts of (1), which corresponds to the equation that the error satisfies at each iteration.

Lemma 1 (Local solutions). *The local solutions of (1) with $\mathbf{J} = 0$, computed in Fourier space, are given by*

$$\mathcal{F}(\mathbf{E}^1) = e^{\lambda x} \left(-\frac{i(A_2 k_z + A_4 k_y)}{\lambda}, A_4, A_2 \right)^T, \quad \mathcal{F}(\mathbf{E}^2) = e^{-\lambda x} \left(\frac{i(A_1 k_z + A_3 k_y)}{\lambda}, A_3, A_1 \right)^T \quad (7)$$

where $\lambda = \sqrt{|\mathbf{k}|^2 - \omega^2}$ and the coefficients $A_{1,2,3,4}$ may depend on k_y, k_z .

The expressions of the solutions in Lemma 1 suggest a different formulation in another basis, which we call the TE-TM decomposition. It can easily be obtained by splitting the solution in (7) into combinations of solutions verifying $A_2 k_z + A_4 k_y = 0$, $A_2, A_4 \neq 0$ (TE modes) and $A_2 k_y = A_4 k_z$, $A_2, A_4 \neq 0$ (TM modes).

Lemma 2 (Local solution decomposition into TE-TM modes). *The local solutions in (7) can be re-written as*

$$\mathcal{F}(\mathbf{E}^j) = A_{TM} \mathcal{F}(\mathbf{E}^{j,TM}) + A_{TE} \mathcal{F}(\mathbf{E}^{j,TE}), \quad j = 1, 2, \quad (8)$$

where

$$\begin{aligned} \mathcal{F}(\mathbf{E}^{1,TE}) &= e^{\lambda x} \left(0, -\frac{k_z}{k_y}, 1 \right)^T, \quad \mathcal{F}(\mathbf{E}^{1,TM}) = e^{\lambda x} \left(-\frac{i|\mathbf{k}|^2}{k_y \lambda}, 1, \frac{k_z}{k_y} \right)^T, \\ \mathcal{F}(\mathbf{E}^{2,TE}) &= e^{-\lambda x} \left(0, -\frac{k_z}{k_y}, 1 \right)^T, \quad \mathcal{F}(\mathbf{E}^{2,TM}) = e^{-\lambda x} \left(\frac{i|\mathbf{k}|^2}{k_y \lambda}, 1, \frac{k_z}{k_y} \right)^T. \end{aligned} \quad (9)$$

To derive the convergence factors, we compute the action of the interface operators from (6), and then replace them into the interface iterations of (1). This calculation is greatly simplified with the decomposition into TE-TM modes, with the difference that we now iterate on the unknowns A_{TE} and A_{TM} . The convergence factor is again given by the spectral radius of some iteration matrix, as in [6], and this matrix happens to be conveniently diagonal for a certain choice of the parameters.

Theorem 1 (Convergence factor for the TE-TM decomposition). *In the case $\delta_3 = \delta_2$, $\delta_4 = \frac{1}{\delta_1}$, which holds for all algorithms we consider, the interface iteration can be written as*

$$\begin{bmatrix} A_{TE} \\ A_{TM} \end{bmatrix}^{1,n} = B \begin{bmatrix} A_{TE} \\ A_{TM} \end{bmatrix}^{1,n-2},$$

with the interface iteration matrix B given by

$$B = \frac{\lambda - i\omega}{\lambda + i\omega} \begin{bmatrix} -\frac{(\lambda+i\omega)(\lambda v_2 \delta_1 + i\omega v_1 \delta_1) + 1}{(\lambda-i\omega)(-\lambda v_2 \delta_1 + i\omega v_1 \delta_1) - 1} & 0 \\ 0 & \frac{(\lambda+i\omega)(\lambda v_1 \delta_1 \delta_2 + i\omega v_2) + \delta_1}{(\lambda-i\omega)(-\lambda v_1 \delta_1 \delta_2 + i\omega v_2) - \delta_1} \end{bmatrix} e^{-2\lambda L}. \quad (10)$$

The proof can be found in [5]. The convergence factor of the algorithm is for each Fourier mode given by the spectral radius of B . In the following we assume that there is no overlap, $L = 0$.

Corollary 1 (DGG conditions). *If we choose $\delta_1 = 1$, $\delta_2 = 1$, $v_1 = v_2 = \frac{1}{|\mathbf{k}|^2 - 2\omega^2 + 2i\omega s}$ in (10), where s is a complex parameter to be chosen, we obtain an iteration matrix with the same convergence factor as in the first order formulation in [6],*

$$\rho_{DGG}(|\mathbf{k}|, \omega, s) = \left| \frac{\sqrt{|\mathbf{k}|^2 - \omega^2 - i\omega}}{\sqrt{|\mathbf{k}|^2 - \omega^2 + i\omega}} \cdot \frac{\sqrt{|\mathbf{k}|^2 - \omega^2 - s}}{\sqrt{|\mathbf{k}|^2 - \omega^2 + s}} \right|. \quad (11)$$

Corollary 2 (RL conditions). *If we choose $\delta_1 = 1$, $\delta_2 = 0$, $v_1 = \frac{1}{\omega^2 + \omega \tilde{k}^{tm}}$, $v_2 = \frac{1}{\omega^2 + \omega \tilde{k}^{te}}$ in (10), where \tilde{k}^{tm} and \tilde{k}^{te} are real parameters to be chosen, we obtain an iteration matrix with convergence factor as in [16],*

$$\rho_{RL}(|\mathbf{k}|, \omega, \tilde{k}^{te}, \tilde{k}^{tm}) = \left| \frac{\sqrt{|\mathbf{k}|^2 - \omega^2 - i\omega}}{\sqrt{|\mathbf{k}|^2 - \omega^2 + i\omega}} \right| \cdot \max \left(\left| \frac{\sqrt{|\mathbf{k}|^2 - \omega^2 - i\tilde{k}^{te}}}{\sqrt{|\mathbf{k}|^2 - \omega^2 + i\tilde{k}^{te}}} \right|, \left| \frac{\sqrt{|\mathbf{k}|^2 - \omega^2 - i\tilde{k}^{tm}}}{\sqrt{|\mathbf{k}|^2 - \omega^2 + i\tilde{k}^{tm}}} \right| \right). \quad (12)$$

Corollary 3 (TETM conditions). *If we choose $\delta_1 = \frac{i\omega + s^{te}}{i\omega + s^{tm}}$, $\delta_2 = 1$, $v_1 = -v_2 = \frac{1}{|\mathbf{k}|^2 - 2\omega^2 + i\omega(s^{te} + s^{tm})}$ in (10), where s^{tm} and s^{te} are real parameters to be chosen, we obtain an iteration matrix with convergence factor as in [14],*

$$\rho_{TETM}(|\mathbf{k}|, \omega, s^{tm}, s^{te}) = \left| \frac{\sqrt{|\mathbf{k}|^2 - \omega^2 - i\omega}}{\sqrt{|\mathbf{k}|^2 - \omega^2 + i\omega}} \right| \cdot \max \left\{ \left| \frac{\sqrt{|\mathbf{k}|^2 - \omega^2 - s^{te}}}{\sqrt{|\mathbf{k}|^2 - \omega^2 + s^{te}}} \right|, \left| \frac{\sqrt{|\mathbf{k}|^2 - \omega^2 - s^{tm}}}{\sqrt{|\mathbf{k}|^2 - \omega^2 + s^{tm}}} \right| \right\}. \quad (13)$$

It remains to explain the choice of the parameters in the three different algorithms: for the DGG conditions, the same choice as for the first order formulation can be used. Minimizing the maximum over all relevant frequencies leads for example in [6, case 3, section 3.5] to

$$s = (1 + i)\sqrt{k_-^{max}}(\omega^2 - k_-^2)^{1/4}/\sqrt{2}, \quad (14)$$

with $k_-^{max} = \frac{c}{h}$ and k_- an estimate of the closest numerical frequency to ω .

For the RL conditions, the authors in [16, 13] recommend

$$\tilde{k}^{te} = -i\sqrt{\left(\frac{1}{2}(k_-^{max,te} + \omega)\right)^2 - \omega^2}, \quad \tilde{k}^{tm} = -i\sqrt{\left(\frac{1}{2}(k_-^{max,tm} + \omega)\right)^2 - \omega^2}, \quad (15)$$

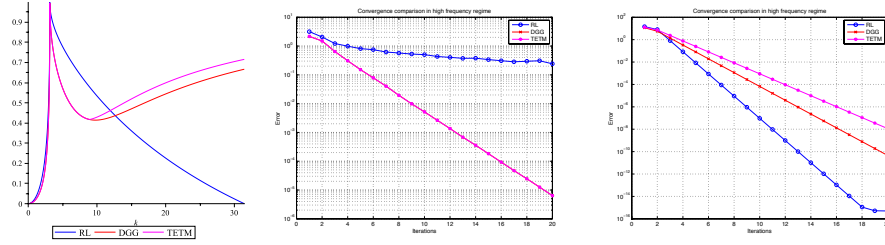


Fig. 1 Comparison of the theoretical contraction factors (11), (12), and (13) on the left, and convergence histories of the corresponding algorithms, in the middle with a random initial guess, and on the right with a high frequency initial guess

with the same estimates $k^{max,te}$, $k^{max,tm}$ as in the TETM case, where a separate minimization of the maximum leads to the parameters

$$s^{te} = (1+i)\sqrt{k^{max,te}}(\omega^2 - k_-^2)^{1/4}/\sqrt{2}, s^{tm} = (1+i)\sqrt{k^{max,tm}}(\omega^2 - k_-^2)^{1/4}/\sqrt{2}. \quad (16)$$

For a mixed type Nedelec elements on irregular tetrahedral meshes, numerical observations in [15, Section 4.5.1] indicate that a good choice is $k^{max,te} = k^{max}$, $k^{max,tm} = \frac{2}{3}k^{max}$. If however $k^{max,te} = k^{max,tm}$, as it is for example the case in a Yee discretization, then minimizing the maximum of the contraction factor in TETM leads again to the DGG transmission conditions. Note that a separate optimization for the TE and TM modes can also potentially be beneficial if one knows for example a priori which TE or TM modes one wants to simulate, since one can then optimize the performance of the algorithm for these modes.

4 Numerical results

We first show a comparison of the theoretical convergence factors ρ_{RL} , ρ_{DGG} and ρ_{TETM} in Figure 1 on the left for the specific values $h = 0.001$ and $\omega = 10\pi$. From these convergence factors, we can expect that a numerical implementation of the algorithm with all error frequencies contained in the initial guess will overall converge better with the DGG and TETM conditions than with the RL conditions. The DGG and TETM transmission conditions have identical convergence behavior for lower error frequencies, but for high error frequencies, the DGG conditions are better. Even though being much less favorable in general, the RL conditions are excellent for very high frequency evanescent error modes.

We now illustrate our convergence results with numerical experiments. We first solve Maxwell's equations in the curl-curl formulation on the domain $\Omega = (0, \pi)^2 \times (0, 2\pi)$ using a Yee scheme. We decompose the domain into two subdomains $\Omega_1 = (0, \pi)^2 \times (0, \pi)$ and $\Omega_2 = (0, \pi)^2 \times (\pi, 2\pi)$. We chose the frequency $\omega = 1$ for this experiment. We show in Figure 1 in the middle and on the right the convergence

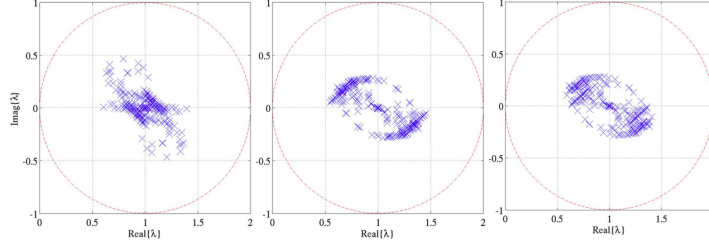


Fig. 2 Eigenspectra for a parallel plate waveguide, $h = \lambda_0/4$, $p = 2$, RL (left), DGG (middle), TETM (right)

histories for the three Schwarz algorithms we considered over 20 iterations. In the middle, we used a random initial guess to make sure all frequencies are present in the error. Here the DGG and TETM algorithms have identical convergence behavior, while the RL algorithm is very slow as expected from the theoretical result in the left plot. On the right we used the highest possible frequency that can be represented on the mesh only as the initial guess for the error. Now, the RL conditions lead to the fastest convergence, whereas the TETM conditions are the slowest, again as expected from the theoretical plot on the left. This shows that one has to be careful when doing numerical investigations: from the right panel in Figure 1, one could conclude that the RL conditions are the best, but this only holds for one particular error frequency. This is why one solves min-max problems to determine optimized parameters: the algorithm needs to be good for all error frequencies uniformly, see especially the experiments in [9, Section 5.1, Figure 5.2].

Next, we show numerical experiments for a discretization with mixed type Nedelec elements on irregular tetrahedral grids. We start by examining the eigenvalues of three non-overlapping domain decomposition matrices, using the RL, DGG, and TETM conditions. We chose a $0.5\lambda_0$ (λ_0 denotes the free space wavelength) segment of a parallel plate waveguide with both ports terminated by first order absorbing boundary conditions. The parallel plate waveguide is partitioned by a transverse plane into two equally sized sub-domains. The mesh size is chosen to be $\lambda_0/4$. In Figure 2, we show the eigenvalue distributions of the three iteration matrices using the RL, DGG, and TETM transmission conditions. All of them provide desirable convergence properties, since all the eigenvalues are within the shifted-unit-circle. It is clear that the spectral radius of the DGG conditions is slightly smaller than the RL conditions, due to the fact that $\rho_{\text{DGG}}^{\max} < \rho_{\text{RL}}^{\max}$. We also see that for this discretization, the TETM conditions further improve the convergence factor of the TM modes: one portion of eigenvalues moves towards the center of the unit circle.

We now present scalability studies: we denote by d the size of the sub-domains, by D the size of the entire problem domain and by h the mesh size. A Krylov subspace iterative method, Generalized Conjugate Residual (GCR) [7], is used for the solution of the matrix equation.

Scalability with respect to ωh : we simulate a $1.5\lambda_0$ segment of a parallel plate waveguide. The waveguide is partitioned into three sub-domains, each $0.5\lambda_0$ long.

Table 1 Number of iterations to attain a relative residual reduction of 10^{-8} for different transmission conditions and different mesh sizes

Cases	$\omega h = 1.57$	$\omega h = 0.785$	$\omega h = 0.524$	$\omega h = 0.393$
RL conditions	23 (19)	27 (17)	34 (22)	41 (22)
DGG conditions	21 (18)	26 (21)	32 (19)	39 (20)
TETM conditions	21 (14)	25 (15)	30 (12)	36 (14)

These sub-domains are meshed independently and quasi-uniformly such that the interface meshes do not match. The mesh size varies from $h = \lambda_0/4$ to $h = \lambda_0/16$. The numbers of iterations required using the RL, DGG, and TETM transmission conditions are given in Table 1, for a random initial guess, and in parentheses with the TEM mode as an excitation and a zero initial guess. The h -refinement permits the representation of more high frequency evanescent modes on the interface, and we see that computing just one TEM mode solution with a zero initial guess requires much less iterations than when all modes are present. The iteration numbers could still substantially be lowered in the one TEM mode case by optimizing just for that mode.

Scalability with respect to ωD : We fix the subdomain size to $0.3\lambda_0$, and we increase the length of the waveguide by increasing the number of subdomains. The mesh size is kept fixed as well at $h = \lambda_0/8$. The performance of the methods for 10, 20, 40, and 80 subdomains is shown in Table 2, again for a random initial guess, and then in parentheses with the TEM mode as excitation, and a zero initial guess. In this study, the propagating modes are of pre-dominant significance since the wave must travel from one end of the waveguide to the other. We see that all of the three conditions show dependence on the problem size, which is expected in the absence of a coarse space. We see that the DGG and TETM conditions perform much better in this set of experiments than the RL condition, and also that all methods need a substantially bigger number of iterations in the presence of all error modes, than when just one mode is present.

5 Conclusions

We have shown that the optimized transmission conditions developed for the first order Maxwell system in [6] can also be used for the curl-curl formulation, and

Table 2 Number of iterations to attain a relative residual reduction of 10^{-8} for different transmission conditions and different problem sizes

Cases	$\omega D = 18.8$	$\omega D = 37.7$	$\omega D = 75.3$	$\omega D = 150.7$
RL conditions	34 (17)	63 (28)	146 (72)	363 (168)
DGG conditions	30 (18)	49 (22)	90 (33)	185 (51)
TETM conditions	31 (21)	46 (22)	85 (29)	176 (37)

the corresponding convergence factors and hence optimized parameters are identical. We illustrated these results with a Yee discretization of the curl-curl formulation. We then showed also numerical experiments with a mixed type Nedelec finite element discretization on irregular tetrahedral grids, and presented several scaling experiments.

References

1. Alonso-Rodriguez, A., Gerardo-Giorda, L.: New nonoverlapping domain decomposition methods for the harmonic Maxwell system. *SIAM J. Sci. Comput.* **28**(1), 102–122 (2006)
2. Chevalier, P., Nataf, F.: An OO2 (Optimized Order 2) method for the Helmholtz and Maxwell equations. In: 10th International Conference on Domain Decomposition Methods in Science and in Engineering, pp. 400–407. AMS, Boulder, Colorado, USA (1997)
3. Collino, P., Delbue, G., Joly, P., Piacentini, A.: A new interface condition in the non-overlapping domain decomposition for the Maxwell equations. *Comput. Methods Appl. Mech. Engrg.* **148**, 195–207 (1997)
4. Després, B., Joly, P., Roberts, J.: A domain decomposition method for the harmonic Maxwell equations. In: *Iterative methods in linear algebra*, pp. 475–484. North-Holland, Amsterdam (1992)
5. Dolean, V., Gander, M.J., Lee, J.F., Peng, Z.: Optimized Schwarz methods for solving the curl-curl time-harmonic Maxwell equations. in preparation (2013)
6. Dolean, V., Gerardo-Giorda, L., Gander, M.J.: Optimized Schwarz methods for Maxwell equations. *SIAM J. Scient. Comp.* **31**(3), 2193–2213 (2009)
7. Eisenstat, S., Elman, H., Schultz, M.: Variational iterative methods for nonsymmetric systems of linear equations. *SIAM Journal on Numerical Analysis* **20**(2), 345–357 (1983)
8. El Bouajaji, M., Dolean, V., Gander, M.J., Lanteri, S.: Optimized Schwarz methods for the time-harmonic Maxwell equations with damping. *SIAM J. Scient. Comp.* **34**(4), 2048–2071 (2012)
9. Gander, M.J.: Schwarz methods over the course of time. *Electronic Transactions on Numerical Analysis* **31**, 228–255 (2008)
10. Gander, M.J., Magoulès, F., Nataf, F.: Optimized Schwarz methods without overlap for the Helmholtz equation. *SIAM J. Sci. Comput.* **24**(1), 38–60 (2002)
11. Lee, S.C., Vouvakis, M., Lee, J.F.: A non-overlapping domain decomposition method with non-matching grids for modeling large finite antenna arrays. *J. Comput. Phys.* **203**(1), 1–21 (2005)
12. Nedelec, J.C.: *Acoustic and electromagnetic equations. Integral representations for harmonic problems.* Applied Mathematical Sciences, 144. Springer Verlag (2001)
13. Peng, Z., Lee, J.F.: Non-conformal domain decomposition method with second-order transmission conditions for time-harmonic electromagnetics. *J. Comput. Phys.* **229**(16), 5615–5629 (2010)
14. Peng, Z., Rawat, V., Lee, J.F.: One way domain decomposition method with second order transmission conditions for solving electromagnetic wave problems. *J. Comput. Phys.* **229**(4), 1181–1197 (2010)
15. Rawat, V.: Finite element domain decomposition with second order transmission conditions for time-harmonic electromagnetic problems. Ph.D. thesis, Ohio State University (2009)
16. Rawat, V., Lee, J.F.: Nonoverlapping domain decomposition with second order transmission condition for the time-harmonic Maxwell’s equations. *SIAM J. Sci. Comput.* **32**(6), 3584–3603 (2010)